Increased Efficiency of Fatty Acid Uptake Contributes to Lipid Accumulation in Skeletal Muscle of High Fat–Fed Insulin-Resistant Rats

Bronwyn D. Hegarty, Gregory J. Cooney, Edward W. Kraegen, and Stuart M. Furler

In humans and animal models, increased lipid content of skeletal muscle is strongly associated with insulin resistance. However, it is unclear whether this accumulation is due to increased uptake or reduced utilization of fatty acids (FAs). We used ^{3}H-R-bromopalmitate tracer to assess the contribution of tissue-specific changes in FA uptake to the lipid accumulation observed in tissues of insulin-resistant, high fat–fed rats (HFF) compared with control rats (CON) fed a standard diet. To study FA metabolism under different metabolic states, tracer was infused under basal conditions, during hyperinsulinemic-euglycemic clamp (low FA availability) or during the infusion of intralipid and heparin (high FA availability). FA clearance was significantly increased in the red gastrocnemius muscle of HFF under conditions of low (HFF = 10.4 ± 1.1; CON = 7.4 ± 0.5 ml · min^{-1} · 100 g^{-1}; $P < 0.05$), basal (HFF = 8.3 ± 1.4; CON = 4.5 ± 0.7 ml · min^{-1} · 100 g^{-1}; $P < 0.01$), and high (HFF = 7.0 ± 0.8; CON = 4.3 ± 0.5 ml · min^{-1} · 100 g^{-1}; $P < 0.05$) FA levels. This indicates an adaptation by muscle for more efficient uptake of lipid. Associated with the enhanced efficiency of FA uptake, we observed increases in CD36/FA translocase mRNA expression ($P < 0.01$) and acyl-CoA synthetase activity ($P < 0.02$) in the same muscle. FA clearance into white adipose tissue was also increased in HFF when circulating FA were elevated, but there was little effect of the high-fat diet on hepatic FA uptake. In conclusion, insulin resistance induced by feeding rats a high-fat diet is associated with tissue-specific adaptations that enhance utilization of increased dietary lipid but could also contribute to the accumulation of intramuscular lipid with a detrimental effect on insulin action. *Diabetes* 51: 1477–1484, 2002

From the Diabetes and Metabolism Research Program, Garvan Institute of Medical Research, Sydney, Australia.

Address correspondence and reprint requests to Stuart Furler, PhD, Garvan Institute of Medical Research, St. Vincent's Hospital, 384 Victoria St., Sydney NSW 2010. E-mail: s.furler@garvan.org.au.

Received for publication 26 June 2001 and accepted in revised form 30 January 2002.

ACS, acyl-CoA synthetase; FA, fatty acid; LCACoA, long-chain acyl-CoA; PKC, protein kinase C; WAT, white adipose tissue.

It is now clear that insulin resistance is not solely a disorder of carbohydrate metabolism but also involves alterations in lipid metabolism (1). Increased adiposity and accumulation of lipid within the liver and skeletal muscle have been shown to be strongly associated with insulin resistance (2). The response of skeletal muscle to insulin greatly influences whole-body insulin sensitivity because it is the main tissue responsible for insulin-stimulated glucose uptake (3). Studies in humans (4–8) and various animal models (9–14) have demonstrated a strong relationship between muscle lipid content and insulin resistance, both at the whole-body level and within the skeletal muscle itself. Intramuscular accumulation of lipid could impinge on the insulin sensitivity of muscle through a number of mechanisms, including substrate competition (15), alteration of insulin signaling (16–19), and/or inhibition of enzymes involved in carbohydrate metabolism (20). However, the processes that control the accumulation of lipid within the muscle are unknown. It is unclear whether lipid accumulates mainly due to an increase in the uptake of non-esterified fatty acids (FAs) or a reduction in their utilization as a fuel (21).

The aim of the current study was to use the recently developed FA tracer [9,10-^{3}H]-(R)-2-bromopalmitate (^{3}H-R-BrP) to determine how lipid metabolism is altered in rats made insulin resistant by intake of a high-fat diet for 3 weeks. The ^{3}H-R-BrP methodology allows tissue-specific measurement of FA uptake and when used in conjunction with ^{14}C-palmitate (^{14}C-P) also provides information on the fate of FAs after entry into the cell (22,23). The effect of high-fat feeding on FA uptake and fate was investigated in the main tissues important in lipid handling and insulin resistance: oxidative skeletal muscle, white adipose tissue (WAT), and liver. The results show that there are significant changes in the FA uptake pathway in red gastrocnemius muscle of high fat–fed rats. These changes would increase the efficiency of the tissue to incorporate available dietary lipid but could also contribute to lipid accumulation in skeletal muscle with detrimental effects on insulin action.

RESEARCH DESIGN AND METHODS

Animals. The experiments were conducted with the approval of the Garvan Institute/St. Vincent's Hospital Animal Experimentation Ethics Committee, following guidelines issued by the National Health and Medical Research Council (Australia).

Experiments were performed on male Wistar rats purchased from Animal Resources Center (Perth, Western Australia). Rats were housed in a temperature-controlled (22 ± 1°C) environment with a 12:12-h light:dark cycle (lights on at 0600 h) with free access to commercial rodent standard diet (Norco, Kempsey, Australia) and water until commencement of diet treatment. Rats were randomly assigned to isocaloric standard diet or high-fat diet groups 3 weeks before study. The macronutrient composition of the diets expressed as a percentage of total dietary calories were as follows: standard diet: 18% fat, 33% protein, and 48% carbohydrate; high-fat diet: 59% fat, 21% protein, and 20% carbohydrate.

Surgery. Chronically indwelling cannulae were inserted into a jugular vein and carotid artery as previously described (24). Anesthesia was induced with 5% and maintained with 1–2% halothane in oxygen. Cannulae were exteriorized dorsally midway between the shoulder blades and ears and were kept patent by filling with polyvinylpyrrolidone until time of study. Suture lines were infiltrated with bupivacaine (0.5 mg/100 g). Buprenorphine was administered subcutaneously (0.003 mg/100 g) postoperatively. After surgery, rats were housed in individual cages and allowed to recover for 7–10 days.

Treatment before tracer administration. Rats received their normal diet on the evening before experiments. To assess FA metabolism across a range of substrate availability, tracer was infused under basal conditions, during hyperinsulinemic-euglycemic clamp, which reduces FA availability, or during infusion of triglyceride emulsion (Intralipid) and heparin, which elevates FA availability.

Rats that underwent hyperinsulinemic-euglycemic clamp were infused with insulin (Actrapid; Novo Nordisk, Copenhagen, Denmark) via the jugular cannula at a constant rate of 0.25 units · kg^{-1} · h^{-1} together with a variable rate of 30% glucose to maintain euglycemia (25). ^{3}H-R-BrP and ^{14}C-P tracers were infused once euglycemia was achieved at ~90 min after initiation of insulin infusion.

The intralipid and heparin infusion was used to raise circulating FAs to similar concentrations in both diet groups. To match plasma lipid concentrations, it was necessary to infuse intralipid at twice the concentration in high fat–fed rats (HFF; 20%) than was required in control rats (CON; 10%) fed the standard diet. Intralipid was mixed with heparin (71.5 units/ml) and infused at a constant rate of 1.3 ml/h via the jugular cannula.

Tracer administration. A mixture of ^{3}H-R-BrP and [U-^{14}C]-palmitate (^{14}C-P) was administered to the rats. The ^{3}H-R-BrP tracer was supplied by AstraZeneca (Mölndal, Sweden). The synthesis of racemic [9,10-^{3}H]-2-bromopalmitic acid and subsequent resolution of the R-isomer has been previously described (22). The ^{14}C-P tracer was commercially available (Dupont, Boston, MA). Each rat was infused with ~25×10^6 dpm ^{3}H-R-BrP and 13×10^6 dpm ^{14}C-P in 1 ml vehicle. Tracer was delivered in saline conjugated with BSA (22) and was infused at a constant rate into the jugular cannula of conscious rats over a 4-min period.

Plasma samples. Arterial blood samples (~400 μl) were collected at baseline and directly before tracer administration. Smaller samples (~200 μl) were also taken at 5-min intervals during infusion of intralipid and heparin and at 1, 2, 3, 4, 5, 6, 8, 12, and 16 min after the start of tracer infusion. All blood samples were immediately centrifuged, and the separated plasma was frozen by immersion in liquid nitrogen and stored at −20°C until analyzed. Erythrocytes from the samples taken before tracer administration were resuspended in saline and returned to the animal to minimize blood loss. Throughout the experiment, the arterial cannula was kept patent by a slow constant infusion (0.6 ml/h) of 20 mmol/l sodium citrate in saline.

Tissue samples. After collection of the final blood sample, rats were killed with an overdose (60 mg) of pentobarbitone injected into the carotid cannula. Samples of red gastrocnemius muscle, liver, and epididymal WAT were rapidly dissected, freeze clamped with aluminum tongs precooled in liquid nitrogen, and stored at −70°C before analysis.

Plasma tracer concentrations. The method for isolation of ^{3}H-R-BrP and ^{14}C-P from total ^{3}H and ^{14}C plasma activities has been described previously (22). Briefly, an initial acid lipid extraction, using a mixture of isopropanol-hexane-0.5 mol/l H_2SO_4 (40:10:1) was followed by a polarity separation step under alkaline conditions. The latter procedure predominantly partitioned esterified FAs into a hexane phase and FAs in anionic form (including the ^{3}H-R-BrP and ^{14}C-P tracers) into an alcohol phase. Small corrections (<10%), based on separation of FAs and esterified FA standards, were applied for incomplete partitioning of tracer.

Tissue tracer content. Tissue samples were homogenized in chloroform: methanol (2:1) using a glass homogenizer. An aliquot of this homogenate was taken to determine the total ^{3}H activity. The remaining tissue homogenate was spun at 3,500*g* for 15 min. The resultant supernatant was separated into aqueous and organic phases by the addition of 1 ml distilled water and an additional 10-min spin at 3,500*g*. The ^{14}C activity in the organic phase was used to measure the incorporation of tracer into intracellular lipid pools. Activities of ^{3}H and ^{14}C in appropriate plasma and tissue fractions were measured on a Beckman LS 6000SC liquid-scintillation counter (Beckman Instruments, Fullerton, CA) using a dual label protocol.

Plasma lipids. Plasma FA concentration was determined using an acyl-CoA oxidase–based colorimetric kit (WAKO FA-C; WAKO Pure Chemical Industries, Osaka, Japan). Plasma triglyceride content was measured using an enzymatic colorimetric technique (Peridochrom Triglycerides GPO-PAP; Boehringer Mannheim, Mannheim, Germany).

Tissue triglyceride content. The triglyceride content of red gastrocnemius muscle and liver from basal animals was determined using an high-performance liquid chromatography (HPLC) method adapted from that of Homan and Anderson (26). The organic phase of tissue samples was separated on a Sherisorb S5W silica column (Waters, Milford, MA) using a mobile phase combining three solvent mixtures: *1*) heptane:tetrahydrofurane (99:1, vol/vol); *2*) acetone:dichloromethane (2:1, vol/vol); and *3*) 2-propanol (7.5 mmol/l acetic acid, 7.5 mmol/l ethanolamine, in water; 85:15 vol/vol). Triglycerides were detected using an evaporative light-scattering device (PL-ELS 1000; Polymer Laboratories, Church Stretton, UK) and quantified by measurement of peak area and comparison to known standards using Chromeleon software (version 4.1).

Muscle CD36 mRNA expression. Semiquantitative RT-PCR techniques were used to measure CD36 mRNA expression in red gastrocnemius muscle from additional rats fed a standard or high-fat diet. Total mRNA was isolated using Tri Reagent (Sigma Chemical, St. Louis, MO) and was further purified using RNEasy Mini Kit (Qiagen, Hilden, Germany). cDNA was synthesized with the use of Omniscript reverse transcriptase for first-strand cDNA synthesis (Qiagen) and oligo (dT) primers. PCR primers for the measurement of CD36 (forward: TTG TTC TTC CAG CCA ACG CC; reverse: CCA GTT ATG GGT TCC ACA TCC AAG) and β-actin (forward: AAT CCT GTG GCA TCC ATG AAA C; reverse: CGC AGC TCA GTA ACA GTC CG) were designed to produce amplicons of 256 and 342 bp, respectively. PCR was performed using Amplitaq Gold DNA polymerase (Applied Biosystems, Foster City, CA). Cycle parameters were 94°C for 45 s, 55°C for 30 s, and 72°C for 30 s, with 27 cycles used for β-actin amplification and 32 cycles for CD36. Controls containing either no cDNA or RNA that had not undergone reverse transcription confirmed the lack of contamination from genomic DNA or other sources. PCR products were separated by agarose gel electrophoresis and detected by ethidium bromide staining. The densities of PCR products were quantified using the software packages Molecular Analyst (Bio-Rad Laboratories, Hercules, CA) and NIH Image (National Institutes of Health, Bethesda, MD). CD36 expression was normalized to β-actin expression.

Muscle acyl-CoA synthetase activity. The acyl-CoA synthetase (ACS) activity of red gastrocnemius muscle from basal animals was determined by measuring ^{14}C-palmitate incorporation into palmitoyl-CoA, as previously described (5).

Calculations. The tissue clearance rates of ^{3}H-R-BrP and ^{14}C-P (K_f^* and K_{fs}', respectively) were calculated from the following:

$$K_f^* = \frac{m_B}{\int_0^T C_B(t)dt} \quad ; \quad K_{fs}' = \frac{m_p}{\int_0^T C_p(t)dt} \qquad (1)$$

where m_B is the tissue content of radiolabeled products of ^{3}H-R-BrP, m_P is the tissue content of organic radiolabeled products of ^{14}C-P, C_B and C_P are arterial plasma concentrations of extracted ^{3}H-R-BrP and ^{14}C-P, respectively, and t is the length of the experiment (~16 min).

Integrals were evaluated analytically using regressions of discrete C_B and C_P values to a double exponential impulse response function (22).

Indices of FA utilization were calculated from the following:

$$R_f^* = K_f^* \cdot C_{FA} \quad ; \quad R_{fs}' = K_{fs}' \cdot C_{FA} \qquad (2)$$

where C_{FA} is the plasma concentration of unlabeled FA.

As the radioactive products of ^{3}H-R-BrP are effectively trapped in tissues (22), R_f^* is an index of the total FA uptake. R_{fs}', derived from ^{14}C accumulation, represents uptake to storage products (22). In the present study, we refined our estimates of K_{fs}' and R_{fs}' by using only organic (rather than total) products in their calculation.

K_f^* and R_f^* are proportional to the actual clearance and uptake rates of circulating FAs (22). However, because of different affinities of analog and authentic substrates for key metabolic processes, the constant of proportionality (LC*) is not 1. Appropriate values of LC* for different tissues of the conscious rat have been previously determined (23). In the present study, we wished to quantitatively compare total and storage components of FA uptake. Therefore, the indices of total FA clearance and uptake used here were K_f^*/LC* and R_f^*/LC*, respectively.

As high-fat feeding of rats tends to increase the mass of both liver and

TABLE 1
Body weight, plasma glucose and insulin, and glucose infusion rate

	Control	High fat
Body weight (g)		
basal	350 ± 6	361 ± 7
clamp	355 ± 6	358 ± 5
intralipid	379 ± 7	381 ± 10
Plasma glucose (mmol/l)		
basal	7.3 ± 0.3	8.2 ± 0.3*
clamp	7.3 ± 0.3	7.2 ± 0.2
intralipid	7.2 ± 0.2	7.8 ± 0.3
Plasma insulin (mU/l)		
basal	29.9 ± 5.6	49.3 ± 4.6
clamp	140.1 ± 9.3	133.9 ± 3.4
intralipid	81.7 ± 12.8	107.5 ± 12.9*
Glucose infusion rate		
($mg \cdot kg^{-1} \cdot min^{-1}$) clamp	30.5 ± 2.8	16.1 ± 1.3†

Data are means ± SE for rats studied under basal conditions, during hyperinsulinemic-euglycemic clamp or infusion of intralipid and heparin (n = 6–8 animals/group). Average plasma glucose and insulin concentrations were determined from samples taken directly before and at the end of tracer exposure. The glucose infusion rate was calculated over a period of 60 min during hyperinsulinemic-euglycemic clamp. *$P < 0.05$, †$P < 0.001$ compared with control.

WAT, FA clearance into these tissues was expressed per whole liver and adipose depot, respectively, to reflect their influence on whole-body uptake.

Estimates of whole-body ^{14}C-P clearance and FA disposal (MCR_P and R_P, respectively) were derived from the following:

$$MCR_P = \frac{D}{\int_0^{\infty} C_P(t)dt} \quad ; \quad R_P = MCR_P \cdot C_{FA} \qquad (3)$$

where D is the total dose of ^{14}C-P administered during the 4-min infusion period.

The integral in equation (3) was evaluated as described above for equation (1).

Statistical analysis. Planned contrasts between individual groups were performed using pooled variance estimates derived from one-way ANOVA (Fisher's protected least significant difference). Where appropriate, a log transformation was applied to equalize errors across groups. Calculations were performed using a commercial software package StatView (Abacus Concepts/Brainpower, Berkeley, CA). Results are expressed as means ± SE. $P < 0.05$ was considered statistically significant.

RESULTS

There was no effect of high-fat diet on body weight (HFF: 365.1 ± 4.4 g, n = 21; CON: 363.1 ± 4.5 g, n = 20) reflecting the isocaloric administration of the diets. Under basal conditions, HFF displayed a small but significant increase in plasma glucose concentration ($P < 0.02$), which was associated with slightly elevated plasma insulin levels (NS; Table 1). Similar tendencies were apparent during the infusion of intralipid and heparin, and plasma glucose and insulin levels were well-matched in clamped animals (Table 1). As expected, HFF were insulin-resistant, as indicated by a reduced glucose infusion rate necessary to maintain euglycemia during physiological hyperinsulinemia ($P < 0.001$; Table 1). HFF accumulated triglyceride within the red gastrocnemius muscle (1.44 ± 0.12 vs. 0.81 ± 0.09 mg/g tissue; $P < 0.002$) and liver (31.42 ± 2.44 vs. 7.77 ± 2.07 mg/g tissue; $P < 0.0001$) relative to CON.

Plasma FA levels and whole-body FA turnover. Plasma FA concentrations and indices of whole-body FA metabolism are presented in Table 2. Overall, circulating FA availability was reduced from basal levels during hyperinsulinemic-euglycemic clamp ($P < 0.001$) and increased to the upper end of the physiological range by infusion of intralipid and heparin ($P < 0.0001$; ANOVA of grouped data).

TABLE 2
Whole-body FA metabolism

	Control	High fat
Plasma FA (mmol/l)		
basal	0.36 ± 0.04	0.28 ± 0.03
clamp	0.11 ± 0.01	0.08 ± 0.01
intralipid	1.43 ± 0.08	1.62 ± 0.11*
MCR_P ($ml \cdot min^{-1} \cdot 100\ g^{-1}$)		
basal	7.42 ± 0.48	9.61 ± 1.01*
clamp	10.1 ± 0.6	11.2 ± 0.6
intralipid	7.81 ± 0.59	7.74 ± 0.30
R_P ($\mu mol \cdot min^{-1} \cdot 100\ g^{-1}$)		
basal	2.60 ± 0.23	2.59 ± 0.19
clamp	1.12 ± 0.15	0.94 ± 0.09
intralipid	10.92 ± 0.53	12.42 ± 0.64†

Data are means ± SE for n = 6–8 animals/group. Average plasma FA concentration, whole-body FA clearance (MCR_P), and whole-body FA disposal (R_P) are presented for rats studied under basal conditions, during hyperinsulinemic-euglycemic clamp or infusion of intralipid and heparin. *$P < 0.05$, †$P < 0.01$ compared with control.

HFF showed a small increase in whole-body ^{14}C-P clearance under basal conditions ($P < 0.05$; Table 2) and a similar tendency during hyperinsulinemic-euglycemic clamp (NS). There was no effect of high-fat feeding on whole-body ^{14}C-P clearance detected when circulating FAs were elevated (Table 2). To achieve similar circulating FA concentrations in the two diet groups, it was necessary to infuse HFF with intralipid at twice the rate of CON. It is likely that this reflects an enhanced clearance of infused triglyceride without previous lipolysis, as it is known that a large fraction of triglyceride in artificial emulsions can be cleared without degradation (27).

Whole-body FA disposal was increased in HFF during infusion of intralipid and heparin ($P < 0.01$; Table 2) but under no other condition due to small differences in circulating FA concentrations between diet groups.

Tissue FA clearance. The estimates of tissue FA clearance rates (K_f*/LC) were derived from ^{3}H-R-BrP plasma disappearance curves and tissue ^{3}H accumulation (equation 1). High-fat feeding increased FA clearance into red gastrocnemius muscle under all experimental conditions (Fig. 1*A*). HFF also exhibited increased FA clearance into WAT at the elevated FA concentrations (Fig. 1*B*), but the high-fat diet did not affect FA clearance into the liver under any experimental conditions (Fig. 1*C*). ^{3}H-R-BrP clearance was also measured in the white quadriceps muscle and heart (Table 3). High-fat feeding caused an increase in ^{3}H-R-BrP clearance in white quadriceps muscle and heart under basal and clamped conditions; however, it had no significant effect during infusion of intralipid and heparin.

Tissue FA clearance into storage. FA clearance into storage (K_{fs}') was calculated using the ^{14}C-P plasma disappearance curve and ^{14}C accumulation within the organic phase of the tissue extraction (equation 1). These data describe FAs that, after uptake into the tissue, are

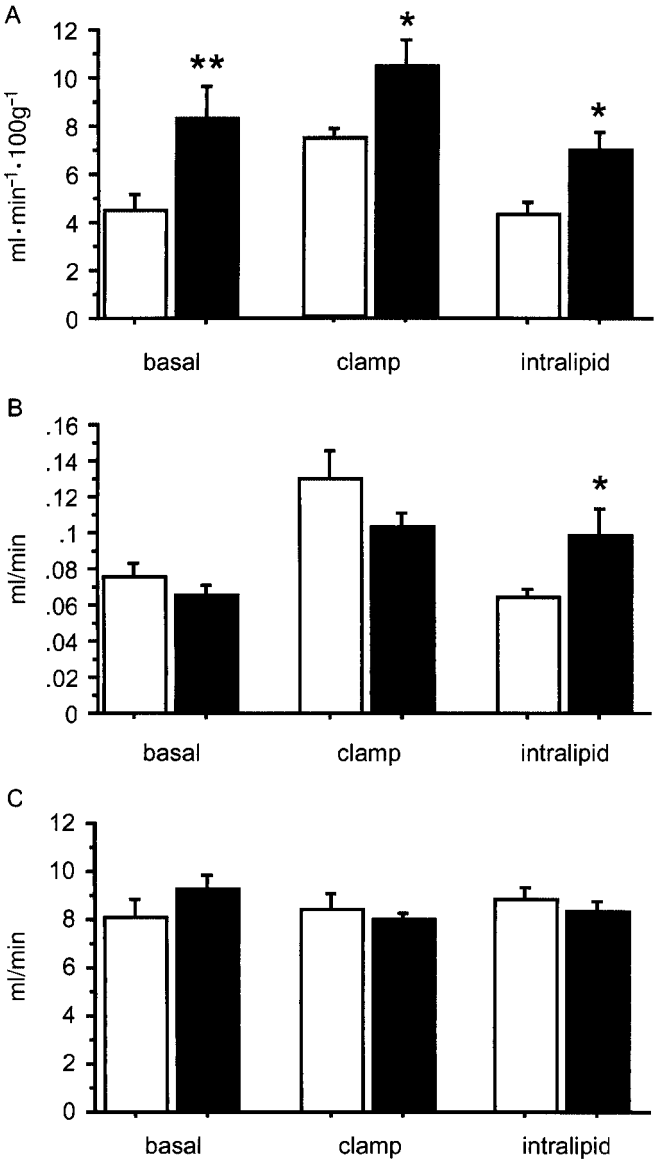

FIG. 1. Indices of FA clearance (K_f*/LC*) into red gastrocnemius muscle (*A*), WAT (*B*), and liver (*C*) in CON (□) and HFF (■) studied under basal conditions, during hyperinsulinemic-euglycemic clamp (clamp) or during infusion of intralipid and heparin (intralipid). Values for WAT and liver are expressed per adipose depot and total liver, respectively. *$P < 0.05$, **$P < 0.01$ compared with CON. Values are means ± SE; $n = 6–8$ animals/group.

stored rather than oxidized or metabolized into nonlipid compounds. HFF showed an increased clearance into storage in red gastrocnemius muscle under conditions of basal and elevated FA availability (Fig. 2*A*), WAT under conditions of increased FA availability (Fig. 2*B*), and liver under basal conditions (Fig. 2*C*). High-fat feeding increased ^{14}C-palmitate clearance into storage in the white quadriceps muscle under all conditions and in the heart under basal conditions (Table 3). ^{14}C-P clearance into storage in the red gastrocnemius muscle correlated with the triglyceride content of that muscle under basal conditions ($r^2 = 0.41$, $P < 0.02$).

Intracellular FA partitioning. To examine whether an alteration in the intracellular FA partitioning between storage and oxidation may contribute to the lipid accumulation in the red gastrocnemius muscle and liver of HFF, the ^{14}C-P clearance/^{3}H-R-BrP clearance ratios (K_{fs}'/(K_f*/LC*) were calculated. These ratios, displayed in Table 4, provide an estimate of the proportion of FA taken up by a tissue that is directed to storage. In the liver, there was a small but significant effect of high-fat feeding to increase the ratio under basal conditions ($P < 0.05$). This indicates that under this condition, FAs may be preferentially directed to storage in the liver of HFF. In muscle, similar ^{14}C-P clearance/^{3}H-R-BrP clearance ratios were found for CON and HFF under all experimental conditions, although there was a nonsignificant tendency for the ratio to be increased in red gastrocnemius muscle of HFF when the FA levels were raised (Table 4).

Red gastrocnemius muscle CD36 mRNA expression and ACS activity. To explore possible mechanisms underlying the increased FA clearance into red gastrocnemius muscle of HFF, we measured the mRNA expression of CD36, a putative FA transporter, and the activity of ACS, the first enzyme of intracellular FA metabolism that catalyzes the activation of FAs to long-chain acyl-CoA (LCA-CoA). Both CD36 mRNA levels ($P < 0.01$) and ACS activity ($P < 0.02$) of the red gastrocnemius muscle were increased in HFF (Fig. 3). Furthermore, ACS activity correlated with both ^{14}C-P clearance into storage ($r^2 = 0.36$, $P < 0.05$) and triglyceride content ($r^2 = 0.49$, $P < 0.02$) of the red gastrocnemius muscle.

DISCUSSION

Although the association between increased muscle lipid content and insulin resistance is well established, the mechanisms behind the lipid accumulation are still a

TABLE 3
Indices of FA clearance (ml · min^{-1} · 100 g^{-1}) and fate in the white quadriceps muscle and heart

	^{3}H-R-BrP clearance		^{14}C-P clearance into storage	
	Control	High fat	Control	High fat
White quadriceps				
basal	1.82 ± 0.17	3.03 ± 0.47*	1.44 ± 0.11	2.18 ± 0.16*
clamp	4.37 ± 0.34	5.89 ± 0.48†	2.76 ± 0.36	3.46 ± 0.29*
intralipid	3.20 ± 0.22	3.60 ± 0.30	1.46 ± 0.14	2.13 ± 0.25*
Heart				
basal	100.7 ± 7.9	119.6 ± 5.9*	12.5 ± 2.7	21.4 ± 3.0*
clamp	91.4 ± 10.3	112.9 ± 5.1*	50.5 ± 8.2	61.8 ± 5.9
intralipid	90.2 ± 3.1	74.7 ± 5.8	17.6 ± 3.4	17.2 ± 2.4

Data are means ± SE for rats studied under basal conditions, during hyperinsulinemic-euglycemic clamp or infusion of intralipid and heparin ($n = 6–10$ animals/group). *$P < 0.05$, †$P < 0.01$ compared with control.

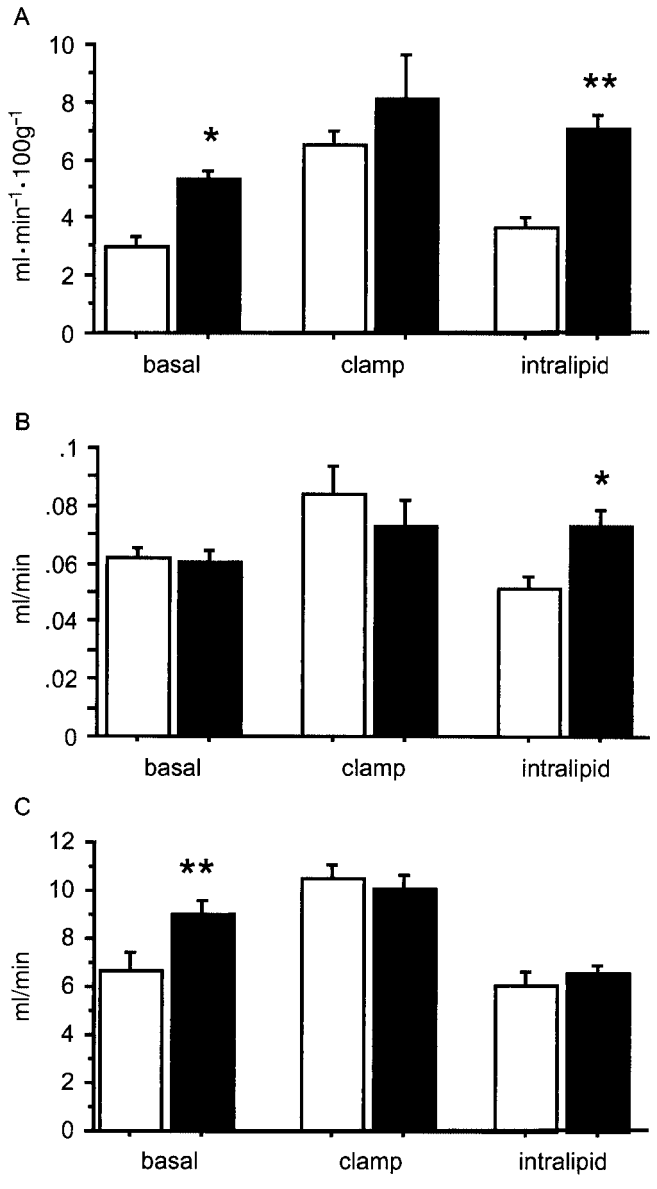

FIG. 2. Indices of FA clearance into storage (K_{fs}') in red gastrocnemius muscle (*A*), WAT (*B*), and liver (*C*) in CON (□) and HFF (■) studied under basal conditions, during hyperinsulinemic-euglycemic clamp (clamp) or during infusion of intralipid and heparin (intralipid). Values for WAT and liver are expressed per adipose depot and total liver, respectively. **$P < 0.01$, ***$P < 0.001$ compared with standard diet. Values are means ± SE; $n = 6–8$ animals/group.

matter of some debate. In this study, we used the recently developed ^{3}H-R-BrP tracer methodology to investigate alterations in FA metabolism that occur when insulin resistance is induced by feeding rats a high-fat diet.

Both the efficiency with which a tissue can take up a substrate (tissue clearance) and availability of the substrate determine the absolute uptake of the substrate into the tissue (equation 2). The increased FA clearance in red gastrocnemius muscle of HFF reported in this study was evident under all experimental conditions and translated into greater absolute FA uptake (R_f*/LC*) across the range of substrate concentrations (Fig. 4). This result suggests that the muscle has undergone intrinsic adaptation such that it can more efficiently use the most abundant energy source available. This enhanced ability of the red gastrocnemius muscle to clear FAs could also contribute to the increased lipid content of the tissue and indicates that lipid accumulation in muscle of HFF does not occur simply because of an increase in the systemic supply of substrate. The increased muscle FA clearance may also be responsible for the tendency toward lower plasma FA concentrations evident in HFF under basal and clamped conditions (Table 2).

Kelley and Goodpaster (21) proposed that the accumulation of triglyceride in muscle associated with insulin resistance is due to a decrease in FA oxidation rather than increased FA uptake. Although this might occur in obese humans (28), we found no evidence in muscle of HFF for a partitioning of FA uptake toward storage and away from oxidation. In a previous study (23), pharmacologic blockade of β-oxidation reduced the clearance of ^{3}H-R-BrP into red skeletal muscle. Therefore, a decrease in ^{3}H-R-BrP clearance might also be expected in HFF if these animals had impaired FA oxidation. However, in the present study, the opposite effect was observed. Moreover, FA clearance and storage were increased proportionately in red gastrocnemius muscle of HFF (Table 4), suggesting that both the storage and oxidation components of FA metabolism were increased in this tissue. This effect is apparently not restricted to our dietary model of insulin resistance. In a recent study of Zucker rats using the perfused hindlimb preparation (29), both FA uptake and oxidation were increased proportionately in obese rats compared with controls, such that the percentage of FA oxidized was similar in insulin-resistant and control groups. There was a tendency in the current study for a greater proportion of FA to be directed to storage in the muscle of HFF when FA levels were raised. Although this difference was not significant, we cannot preclude a minor shift in the intracellular partitioning of FA under these conditions.

To investigate possible mechanisms for the increased efficiency of FA uptake in the red gastrocnemius muscle of HFF, we examined markers of FA transport and activation. As high-fat feeding did not preferentially upregulate either FA storage or oxidation, we chose to investigate early steps of muscle FA metabolism, common to both of these pathways. CD36 (also known as FA translocase) is a membrane protein thought to function as an FA transporter (reviewed in Frohnert and Bernlohr [30] and Abumrad et al. [31]). ACS is the enzyme responsible for activation of FA into LCACoA, the first and committed step of intracellular FA metabolism. The demonstrated increase in CD36 mRNA expression and ACS activity in the red gastrocnemius muscle of HFF suggests that exposure to increased dietary lipid upregulates muscle lipid metabolism and provides a mechanism for the enhanced FA clearance. Greenwalt et al. (32) previously reported an increase in CD36 protein levels in the cardiac tissue of mice fed a high-fat diet, and Fabris et al. (33) found elevated muscle CD36 mRNA expression in lean Zucker rats after 3 h of lipid infusion. However, the present study is the first report linking changes in CD36 mRNA and ACS activity to in vivo measures of FA uptake in the same tissue. It should be noted that the results from the present study were obtained from male rats and may not apply to female rats, as there is recent evidence that some aspects

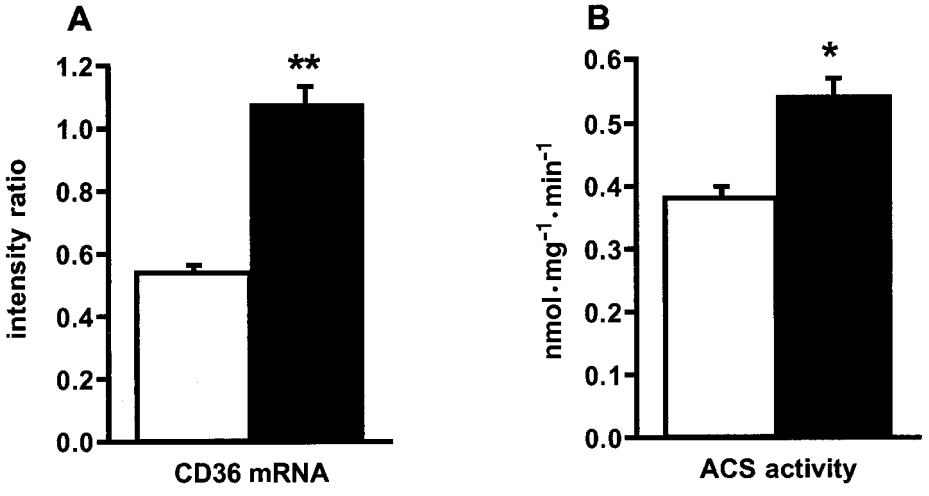

FIG. 3. Expression of CD36 mRNA (normalized for β-actin mRNA expression) (*A*) and ACS activity (*B*) in the red gastrocnemius muscle of CON (□) and HFF (■) studied under basal conditions. **P* < 0.02, ***P* < 0.01 compared with CON. Values are means ± SE; *n* = 6–8 animals/group.

of fat-induced insulin resistance may be sex specific (34,35).

Muscle triglyceride content has been shown to correlate with insulin resistance in many studies and is therefore widely used as a marker of the disorder. However, a mechanism directly linking this correlation with causation of insulin resistance has not been described, and it seems unlikely that triglyceride per se, an inert storage form of lipid, would directly interfere with the action of insulin to stimulate glucose uptake and metabolism. Intermediates of lipid metabolism, such as diglycerides and LCACoA, have also been shown to accumulate in insulin-resistant muscle of HFF (5,36,37). Other than simply being intermediates in lipid utilization, diglycerides and LCACoA are themselves important effector molecules and therefore represent likely candidates for mediating the detrimental effects of lipid accumulation on insulin action. Diglycerides activate conventional and novel protein kinase Cs (PKCs) (38), and increased expression and/or activation of PKCε and/or θ have been associated with reduced insulin action in skeletal muscle in a variety of models of insulin resistance (16,18,39–41). Among other actions, PKCs can interfere with insulin signaling by promoting serine/threonine phosphorylation of insulin receptor substrate-1 via mitogen-activated protein kinase (reviewed in Schmitz-Peiffer [42]). LCACoAs also regulate certain PKCs (43–45) and have been shown to inhibit hexokinase activity in homogenates of rat and human skeletal muscle (20).

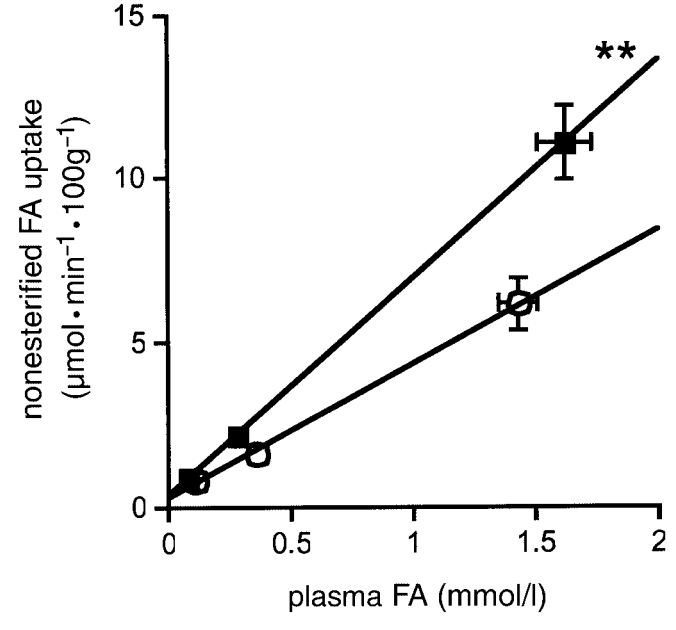

FIG. 4. Estimated FA uptake into skeletal muscle with increasing plasma FA concentration in CON (○) and HFF (■). Values are means ± SE; *n* = 6–8 animals/group.

Two other tissues that are important in FA metabolism were examined in this study for changes in FA utilization. High-fat feeding caused an increase in FA clearance into WAT when FA levels were raised, an adaptation that would serve to improve the capability of HFF to readily dispose of a lipid load. The liver develops insulin resistance after just 3 days of high-fat feeding, evident by a reduced ability of insulin to suppress hepatic glucose output (11,46). There was little effect of the high-fat diet on overall FA uptake into the liver. However, there was evidence that the proportion of FA directed to storage was greater in HFF under basal conditions ($P < 0.05$; Table 3), which could contribute to the hepatic accumulation of triglyceride in these animals (Table 1). Hepatic lipid content is strongly associated with insulin resistance and has been shown to correlate inversely with the ability of insulin to suppress hepatic glucose output (47). The observed alteration in intracellular FA partitioning could be mediated by an increase in activity of enzymes involved in hepatic triglyceride synthesis, such as glycerol-3-phosphate acyl-transferase or the ACS isoforms 1 and 4, which have been shown to be linked specifically with triglyceride

TABLE 4
^{14}C-P clearance/^{3}H-R-BrP clearance ratios ($K_{fs}'/(K_f*/LC*)$)

	Control	High fat
Red gastrocnemius		
basal	0.70 ± 0.08	0.72 ± 0.09
clamp	0.87 ± 0.10	0.74 ± 0.04
intralipid	0.90 ± 0.10	1.09 ± 0.14
Liver		
basal	0.82 ± 0.05	0.99 ± 0.05*
clamp	1.27 ± 0.06	1.27 ± 0.06
intralipid	0.68 ± 0.04	0.80 ± 0.05

Data are means ± SE for rats studied under basal conditions, during hyperinsulinemic-euglycemic clamp or infusion of intralipid and heparin (n = 6–8 animals/group). *$P < 0.05$ compared with control.

synthesis in the liver (48). Alternatively, a decrease in FA oxidation may be responsible. However, it should be noted that this partitioning effect was small and apparent in only one experimental condition and therefore may not be the main mechanism responsible for the marked accumulation of lipid in this tissue. In contrast to skeletal muscle, where we have demonstrated a clear increase in FA clearance that could contribute to the lipid accumulation in that tissue, lipid may well accumulate within the liver simply because of the increase in the supply of substrate to hepatocytes from the diet.

In conclusion, HFF undergo tissue-specific adaptations that allow the available energy source to be more efficiently used and stored. The enhanced ability of skeletal muscle of HFF to extract FA from the circulation, however, is likely to have the detrimental consequence of intramuscular accumulation of lipid intermediates that is associated with the development of insulin resistance.

ACKNOWLEDGMENTS

This work was supported by funding from the National Health and Medical Research Council of Australia. We are grateful to Nick Oakes and Bengt Ljung for helpful discussions regarding this project. We thank Margit Wettesten and Carina Hallberg at AstraZeneca (Mölndal, Sweden) for assistance and use of HPLC system. We appreciate the help of Megan Lim-Fraser with the PCR experiments. We also thank the staff of the Biological Testing Facility at the Garvan Institute for the care of the animals.

REFERENCES

1. McGarry JD: What if Minkowski had been ageusic? An alternative angle on diabetes. *Science* 258:766–770, 1992
2. Kraegen EW, Cooney GJ: The role of free fatty acids in muscle insulin resistance. In *The Diabetes Annual/12*. Marshall SM, Home PD, Rizza RA, Eds. Amsterdam, Elsevier Science B.V., 1999, p. 141–159
3. DeFronzo RA: Lilly lecture 1987. The triumvirate: beta-cell, muscle, liver: a collusion responsible for NIDDM. *Diabetes* 37:667–687, 1988
4. Goodpaster BH, Thaete FL, Kelley DE: Thigh adipose tissue distribution is associated with insulin resistance in obesity and in type 2 diabetes mellitus. *Am J Clin Nutr* 71:885–892, 2000
5. Ellis BA, Poynten A, Lowy AJ, Furler SM, Chisholm DJ, Kraegen EW, Cooney GJ: Long-chain acyl-CoA esters as indicators of lipid metabolism and insulin sensitivity in rat and human muscle. *Am J Physiol Endocrinol Metab* 279:E554–E560, 2000
6. Perseghin G, Scifo P, De Cobelli F, Pagliato E, Battezzati A, Arcelloni C, Vanzulli A, Testolin G, Pozza G, Del Maschio A, Luzi L: Intramyocellular triglyceride content is a determinant of in vivo insulin resistance in humans: a 1H–13C nuclear magnetic resonance spectroscopy assessment in offspring of type 2 diabetic parents. *Diabetes* 48:1600–1606, 1999
7. Pan DA, Lillioja S, Kriketos AD, Milner MR, Baur LA, Bogardus C, Jenkins AB, Storlien LH: Skeletal muscle triglyceride levels are inversely related to insulin action. *Diabetes* 46:983–988, 1997
8. Phillips DI, Caddy S, Ilic V, Fielding BA, Frayn KN, Borthwick AC, Taylor R: Intramuscular triglyceride and muscle insulin sensitivity: evidence for a relationship in nondiabetic subjects. *Metabolism* 45:947–950, 1996
9. Chalkley SM, Hettiarachchi M, Chisholm DJ, Kraegen EW: Five-hour fatty acid elevation increases muscle lipids and impairs glycogen synthesis in the rat. *Metabolism* 47:1121–1126, 1998
10. Laybutt DR, Chisholm DJ, Kraegen EW: Specific adaptations in muscle and adipose tissue in response to chronic systemic glucose oversupply in rats. *Am J Physiol* 273:E1–E9, 1997
11. Oakes ND, Cooney GJ, Camilleri S, Chisholm DJ, Kraegen EW: Mechanisms of liver and muscle insulin resistance induced by chronic high-fat feeding. *Diabetes* 46:1768–1774, 1997
12. Shimabukuro M, Koyama K, Chen G, Wang MY, Trieu F, Lee Y, Newgard CB, Unger RH: Direct antidiabetic effect of leptin through triglyceride depletion of tissues. *Proc Natl Acad Sci U S A* 94:4637–4641, 1997
13. Chen MT, Kaufman LN, Spennetta T, Shrago E: Effects of high fat-feeding to rats on the interrelationship of body weight, plasma insulin, and fatty acyl-coenzyme A esters in liver and skeletal muscle. *Metabolism* 41:564–569, 1992
14. Storlien LH, Jenkins AB, Chisholm DJ, Pascoe WS, Khouri S, Kraegen EW: Influence of dietary fat composition on development of insulin resistance in rats: relationship to muscle triglyceride and omega-3 fatty acids in muscle phospholipid. *Diabetes* 40:280–289, 1991
15. Randle PJ, Garland PB, Hales CN, Newsholm EA: The glucose-fatty acid cycle: its role in insulin sensitivity and the metabolic disturbances of diabetes mellitus. *Lancet* 1:785–789, 1963
16. Griffin ME, Marcucci MJ, Cline GW, Bell K, Barucci N, Lee D, Goodyear LJ, Kraegen EW, White MF, Shulman GI: Free fatty acid-induced insulin resistance is associated with activation of protein kinase C theta and alterations in the insulin signaling cascade. *Diabetes* 48:1270–1274, 1999
17. Zierath JR, Houseknecht KL, Gnudi L, Kahn BB: High-fat feeding impairs insulin-stimulated GLUT4 recruitment via an early insulin-signaling defect. *Diabetes* 46:215–223, 1997
18. Schmitz-Peiffer C, Browne CL, Oakes ND, Watkinson A, Chisholm DJ, Kraegen EW, Biden TJ: Alterations in the expression and cellular localization of protein kinase C isozymes epsilon and theta are associated with insulin resistance in skeletal muscle of the high-fat-fed rat. *Diabetes* 46:169–178, 1997
19. Thompson AL, Lim-Fraser MY, Kraegen EW, Cooney GJ: Effects of individual fatty acids on glucose uptake and glycogen synthesis in soleus muscle in vitro. *Am J Physiol Endocrinol Metab* 279:E577–E584, 2000
20. Thompson AL, Cooney GJ: Acyl-CoA inhibition of hexokinase in rat and human skeletal muscle is a potential mechanism of lipid-induced insulin resistance. *Diabetes* 49:1761–1765, 2000
21. Kelley DE, Goodpaster BH: Skeletal muscle triglyceride. An aspect of regional adiposity and insulin resistance. *Diabetes Care* 24:933–941, 2001
22. Oakes ND, Kjellstedt A, Forsberg GB, Clementz T, Camejo G, Furler SM, Kraegen EW, Olwegard-Halvarsson M, Jenkins AB, Ljung B: Development and initial evaluation of a novel method for assessing tissue-specific plasma free fatty acid utilization in vivo using (R)-2-bromopalmitate tracer. *J Lipid Res* 40:1155–1169, 1999
23. Furler SM, Cooney GJ, Hegarty BD, Lim-Fraser MY, Kraegen EW, Oakes ND: Local factors modulate tissue-specific NEFA utilization: assessment in rats using 3H-(R)-2-bromopalmitate. *Diabetes* 49:1427–1433, 2000
24. Clark PW, Jenkins AB, Kraegen EW: Pentobarbital reduces basal liver glucose output and its insulin suppression in rats. *Am J Physiol* 258:E701–E707, 1990
25. Kraegen EW, James DE, Bennett SP, Chisholm DJ: In vivo insulin sensitivity in the rat determined by euglycemic clamp. *Am J Physiol* 245:E1–E7, 1983
26. Homan R, Anderson MK: Rapid separation and quantitation of combined neutral and polar lipid classes by high-performance liquid chromatography and evaporative light-scattering mass detection. *J Chromatogr B Biomed Sci Appl* 708:21–26, 1998
27. Hultin M, Carneheim C, Rosenqvist K, Olivecrona T: Intravenous lipid emulsions: removal mechanisms as compared to chylomicrons. *J Lipid Res* 36:2174–2184, 1995
28. Kelley DE, Goodpaster B, Wing RR, Simoneau JA: Skeletal muscle fatty acid metabolism in association with insulin resistance, obesity, and weight loss. *Am J Physiol* 277:E1130–E1141, 1999
29. Turcotte LP, Swenberger JR, Zavitz Tucker M, Yee AJ: Increased fatty acid uptake and altered fatty acid metabolism in insulin-resistant muscle of obese Zucker rats. *Diabetes* 50:1389–1396, 2001
30. Frohnert BI, Bernlohr DA: Regulation of fatty acid transporters in mammalian cells. *Prog Lipid Res* 39:83–107, 2000
31. Abumrad N, Coburn C, Ibrahimi A: Membrane proteins implicated in long-chain fatty acid uptake by mammalian cells: CD36, FATP and FABPm. *Biochim Biophys Acta* 1441:4–13, 1999
32. Greenwalt DE, Scheck SH, Rhinehart-Jones T: Heart CD36 expression is increased in murine models of diabetes and in mice fed a high fat diet. *J Clin Invest* 96:1382–1388, 1995
33. Fabris R, Nisoli E, Lombardi AM, Tonello C, Serra R, Granzotto M, Cusin I, Rohner-Jeanrenaud F, Federspil G, Carruba MO, Vettor R: Preferential channeling of energy fuels toward fat rather than muscle during high free fatty acid availability in rats. *Diabetes* 50:601–608, 2001
34. Frias JP, Macaraeg GB, Ofrecio J, Yu JG, Olefsky JM, Kruszynska YT: Decreased susceptibility to fatty acid-induced peripheral tissue insulin resistance in women. *Diabetes* 50:1344–1350, 2001
35. Perseghin G, Scifo P, Pagliato E, Battezzati A, Benedini S, Soldini L, Testolin G, Del Maschio A, Luzi L: Gender factors affect fatty acids-induced insulin resistance in nonobese humans: effects of oral steroidal contraception. *J Clin Endocrinol Metab* 86:3188–3196, 2001

36. Oakes ND, Camilleri S, Furler SM, Chisholm DJ, Kraegen EW: The insulin sensitizer, BRL 49653, reduces systemic fatty acid supply and utilization and tissue lipid availability in the rat. *Metabolism* 46:935–942, 1997
37. Oakes ND, Bell KS, Furler SM, Camilleri S, Saha AK, Ruderman NB, Chisholm DJ, Kraegen EW: Diet-induced muscle insulin resistance in rats is ameliorated by acute dietary lipid withdrawal or a single bout of exercise: parallel relationship between insulin stimulation of glucose uptake and suppression of long-chain fatty acyl-CoA. *Diabetes* 46:2022–2028, 1997
38. Liu WS, Heckman CA: The sevenfold way of PKC regulation. *Cell Signal* 10:529–542, 1998
39. Laybutt DR, Schmitz-Peiffer C, Saha AK, Ruderman NB, Biden TJ, Kraegen EW: Muscle lipid accumulation and protein kinase C activation in the insulin-resistant chronically glucose-infused rat. *Am J Physiol* 277:E1070–E1076, 1999
40. Qu X, Seale JP, Donnelly R: Tissue and isoform-selective activation of protein kinase C in insulin-resistant obese Zucker rats: effects of feeding. *J Endocrinol* 162:207–214, 1999
41. Shafrir E, Ziv E: Cellular mechanism of nutritionally induced insulin resistance: the desert rodent Psammomys obesus and other animals in which insulin resistance leads to detrimental outcome. *J Basic Clin Physiol Pharmacol* 9:347–385, 1998
42. Schmitz-Peiffer C: Signalling aspects of insulin resistance in skeletal muscle: mechanisms induced by lipid oversupply. *Cell Signal* 12:583–594, 2000
43. Majumdar S, Rossi MW, Fujiki T, Phillips WA, Disa S, Queen CF, Johnston RB Jr, Rosen OM, Corkey BE, Korchak HM: Protein kinase C isotypes and signaling in neutrophils: differential substrate specificities of a translocatable calcium- and phospholipid-dependent beta-protein kinase C and a phospholipid-dependent protein kinase which is inhibited by long chain fatty acyl coenzyme A. *J Biol Chem* 266:9285–9294, 1991
44. Nesher M, Boneh A: Effect of fatty acids and their acyl-CoA esters on protein kinase C activity in fibroblasts: possible implications in fatty acid oxidation defects. *Biochim Biophys Acta* 1221:66–72, 1994
45. Orellana A, Hidalgo PC, Morales MN, Mezzano D, Bronfman M: Palmitoyl-CoA and the acyl-CoA thioester of the carcinogenic peroxisome-proliferator ciprofibrate potentiate diacylglycerol-activated protein kinase C by decreasing the phosphatidylserine requirement of the enzyme. *Eur J Biochem* 190:57–61, 1990
46. Kraegen EW, Clark PW, Jenkins AB, Daley EA, Chisholm DJ, Storlien LH: Development of muscle insulin resistance after liver insulin resistance in high-fat-fed rats. *Diabetes* 40:1397–1403, 1991
47. Ryysy L, Hakkinen AM, Goto T, Vehkavaara S, Westerbacka J, Halavaara J, Yki-Jarvinen H: Hepatic fat content and insulin action on free fatty acids and glucose metabolism rather than insulin absorption are associated with insulin requirements during insulin therapy in type 2 diabetic patients. *Diabetes* 49:749–758, 2000
48. Lewin TM, Kim JH, Granger DA, Vance JE, Coleman RA: Acyl-CoA synthetase isoforms 1, 4, and 5 are present in different subcellular membranes in rat liver and can be inhibited independently. *J Biol Chem* 276:24674–24679, 2001